Phase separation of thin SiO layers in amorphous SiO/SiO_2 superlattices during annealing

2003 J. Phys.: Condens. Matter 15 S2887

(http://iopscience.iop.org/0953-8984/15/39/012)

INSTITUTE OF PHYSICS PUBLISHING JOURNAL OF PHYSICS: CONDENSED MATTER

J. Phys.: Condens. Matter **15** (2003) S2887–S2895 PII: S0953-8984(03)67304-2

Phase separation of thin SiO layers in amorphous SiO/SiO_2 superlattices during annealing

L X Yi, J Heitmann, R Scholz and M Zacharias

Max Planck Institute of Microstructure Physics, Weinberg 2, 06120 Halle, Germany

E-mail: lx_yi@yahoo.com

Received 7 August 2003
Published 19 September 2003
Online at stacks.iop.org/JPhysCM/15/S2887

Abstract

The preparation of ordered and arranged Si quantum dots using a SiO/SiO_2 superlattice approach is presented. The different processes of phase separation and crystallization are studied in detail by infrared (IR) absorption and photoluminescence (PL) spectroscopy for different annealing temperatures from 300 to 1100 °C. IR spectra show a continuous shift of the Si–O–Si asymmetric stretching mode to higher energies with increasing annealing temperature, which is a sign of phase separation to Si and SiO_2. Three PL bands are distinguished and correspond to the three processes of phase separation. A band centred at 2.2 eV is present in as-prepared samples and vanishes for annealing above 800 °C which is clearly correlated with defects. The second band shifting from 1.7 to 1.4 eV is detected for annealing temperatures between 300 and 900 °C. A strong red luminescence due to quantum confinement is observed for annealing above 900 °C. Our results indicate that the different and seemingly contradictory PL observations in the literature could originate from different states of network reorganization during the phase separation and crystallization processes. The origins of the different IR and PL bands are discussed in comparison with those of bulk crystalline SiO and SiO_2.

1. Introduction

Bulk crystalline Si is the standard material for semiconductor processing and devices but light emission from this material is highly inefficient due to the indirect nature of the Si band gap. The first report on efficient visible light emission from a Si based material [1, 2] initiated a period of research on the preparation and stabilization of porous Si. Today's silicon nanocrystal research is focused on the preparation of nanocrystals embedded in an oxide host. The methods applied for preparation are Si ion implantation into high quality oxides [3] and the synthesis of Si rich oxides either by sputtering [4] or by reactive evaporation [5]. Using these methods the Si crystal size, determined by the Si content in the SiO_2 matrix, and the crystal density cannot be controlled independently. In addition, there is only limited control of the size distribution itself.

Recently, we developed a new method based on the preparation of SiO/SiO_2 superlattices which allows independent control of position, size and density of the crystals. The Si nanocrystals show a strong room temperature luminescence after crystallization [6]. In this case, the growth of the Si nanocrystals is based on a phase separation and crystallization process within the ultrathin (2–4 nm) SiO layers. During crystallization, different effects, such as the phase separation of the ultrathin amorphous SiO layers including temperature dependent diffusion of Si atoms and the critical crystallization diameter of the Si nanocrystals including the influence of the superlattice structure, i.e. strain, play an important role and are not understood in detail. Diffusion and phase separation processes in confined geometries and growth phenomena in the presence of nearby interfaces have not yet been investigated in any detail.

In this paper, the different processes of phase separation of thin SiO layers in SiO/SiO_2 superlattices will be investigated on the basis of infrared (IR) absorption and photoluminescence (PL) characterization of the films.

2. Experiments

The samples investigated were prepared by alternative evaporation of SiO powder in either vacuum or oxygen atmosphere in order to produce an SiO/SiO_2 superlattice. The evaporation conditions which allow the preparation of size-controlled nc-Si are described elsewhere [6]. The samples investigated have SiO layer thicknesses of 2 nm (sample A) and 4 nm (sample B). The SiO_2 layer thickness for both set of samples is 3 nm. The number of periods is 45. The substrate temperature during growth was 100 °C. For comparison, bulk SiO and SiO_2 layers with 100 nm thickness were prepared under the same conditions. Pieces of the different samples were annealed at selected temperatures between 300 and 1100 °C for 1 h under a nitrogen atmosphere. Every sample was annealed only once.

IR spectroscopy was performed using a FTIR Bruker IFS66v spectrometer equipped with a mercury cadmium telluride IR detector in the range of 600–1500 cm^{-1} and using a plain piece of the same wafer as reference. The PL was excited by the 325 nm line of a HeCd laser. The PL signal was focused into a single monochromator and detected by a nitrogen cooled CCD camera. All spectra were corrected for the spectral response of the measurement system.

3. Results

3.1. FTIR spectroscopy

The IR spectra of the annealing states of sample B (SL 4 nm/3 nm) are presented in figure 1. Various silicon–oxygen related absorption bands can be seen in the range from 700 to 1500 cm^{-1}. The first band around 810 cm^{-1} is assigned to the Si–O–Si bending motion in SiO_2 [7]. For higher annealing temperatures, the second band at 880 cm^{-1} appears with increasing intensity for increasing annealing temperature (T_a) up to 400–500 °C. For higher T_a the absorption band intensity decreases with increasing T_a and vanishes above 700 °C, as shown in figure 2. This band is assigned to silicon ring configurations isolated by oxygen atoms [8–10] or a silicon ring with a non-bridging oxygen hole centre (NBOHC) [11]. The third band above 1000 cm^{-1} is assigned to the asymmetric stretching motion of the oxygen atom of the Si–O–Si bridging configuration. The observed third IR band shifts from 1039 to 1052 cm^{-2} with T_a in the range of 100–600 °C (2.4 cm^{-1}/100 °C; see figure 3). For T_a between 700 and 900 °C, a more pronounced shift (8.5 cm^{-1}/100 °C) is observed which ends at a wavenumber of 1080 cm^{-1} representing the position of SiO_2. Further annealing at higher

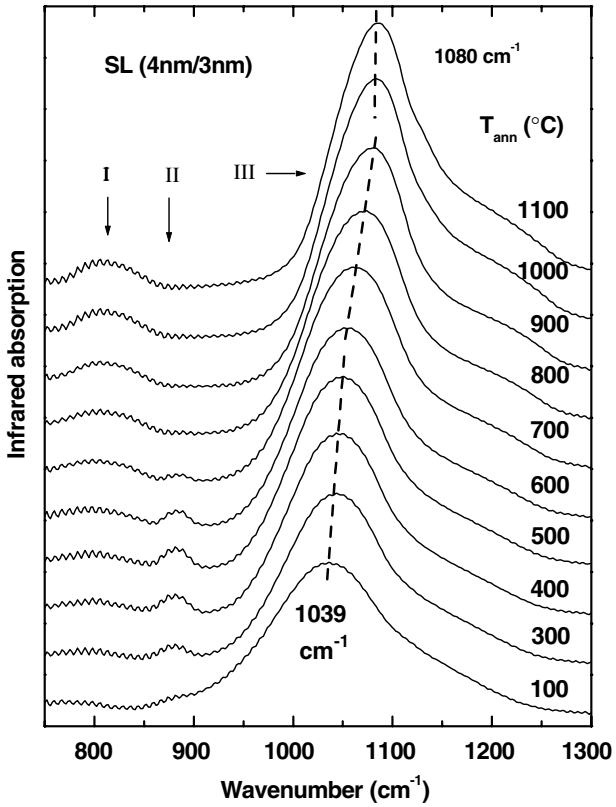

Figure 1. The annealing temperature dependence of the IR spectra for a SiO/SiO$_2$ superlattice (sample B).

temperatures does not result in any shift of the Si–O related bands. The intensity of this band increases and the full width at half-maximum (FWHM) decreases with increasing T_a. The annealing temperature dependences of the absorption bands II and III for the bulk SiO and sample A show a similar tendency to that for sample B (shown in figures 2 and 3). For the bulk SiO film, the IR vibration shift rate is 7.0 cm^{-1}/100 °C in the annealing range from 100 to 600 °C and 14.0 cm^{-1}/100 °C from 700 to 900 °C (see figure 3), which is much faster than for other samples.

The disproportion reaction of SiO_x leads to an oxygen rich suboxide and Si [12]:

$$SiO_x \rightarrow [x/(x+y)]SiO_{(x+y)} + [1 - x/(x+y)]Si \tag{1}$$

with y depending on the specific oxide $SiO_{(x+y)}$. The composition parameter y changes between $y = 0$ at the beginning of the disproportion reaction and $y = 2-x$ when finally the end product SiO_2 has been reached. The gradual increase in the energy value of the Si–O–Si stretching mode (ν_{Si-O}) supports equation (1). The single Si–O stretch peak shape would be expected for either a homogeneous $SiO_{(x+y)}$ alloy or one with concentration gradients. Two distinct Si–O stretch peaks would form if only stoichiometries such as SiO_2 + SiO were formed, which is not observed. To quantify the kinetics of reaction (1), the extent of the reaction (α) can be estimated via

$$y/(2-x) = \alpha \approx (\nu_m - \nu_i)/(\nu_f - \nu_i), \tag{2}$$

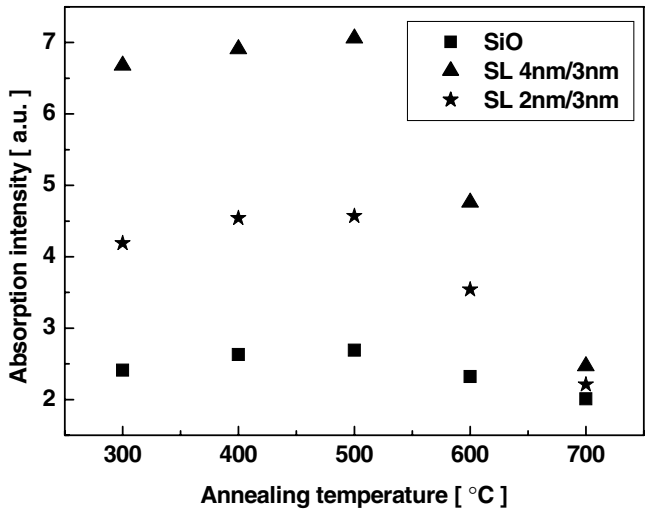

Figure 2. The absorption intensity of IR band II as a function of annealing temperature for SiO/SiO_2 superlattice samples A and B.

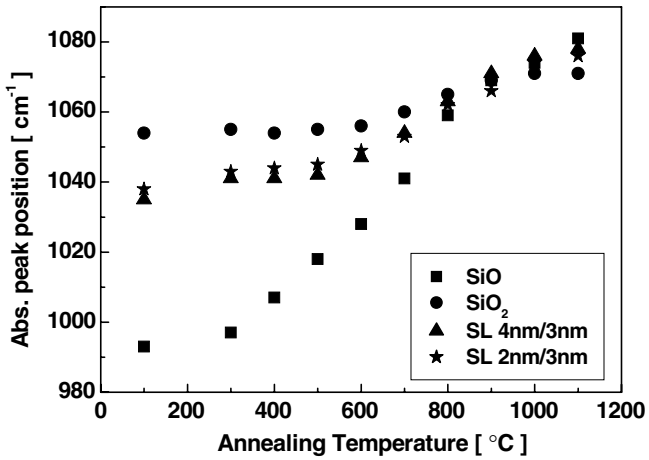

Figure 3. The annealing temperature dependence of the peak position of the Si–O–Si vibration modes (band III) for bulk SiO, SiO_2 and SiO/SiO_2 superlattice samples (samples A and B).

where reaction completion ($\alpha = 1$) is equivalent to $x + y = 2$. ν_m is the measured ν_{Si-O}, ν_i the as-prepared ν_{Si-O} and ν_f the measured ν_{Si-O} at completion (after an annealing at 1100 °C). The integrated area of the Si–O stretch peak remains constant indicating no significant parasitic oxidation. With successive anneals the Si–O stretch peak becomes sharper and higher in frequency as expected in forming SiO_2.

From figure 4, please note that the extent of reaction (α) for the SiO film shows a nearly linear progression of α as a function of the annealing temperature. For the other three samples three stages can be distinguished. At first, the extent of reaction (α) increases slowly with T_a from 300 to 500 °C. For annealing between 600 and 900 °C, α increases pronouncedly as expected in forming SiO_2. Above 900 °C, a nearly constant α indicates no significant oxidation. These results are in good agreement to those of Hinds *et al* [12], proposing that

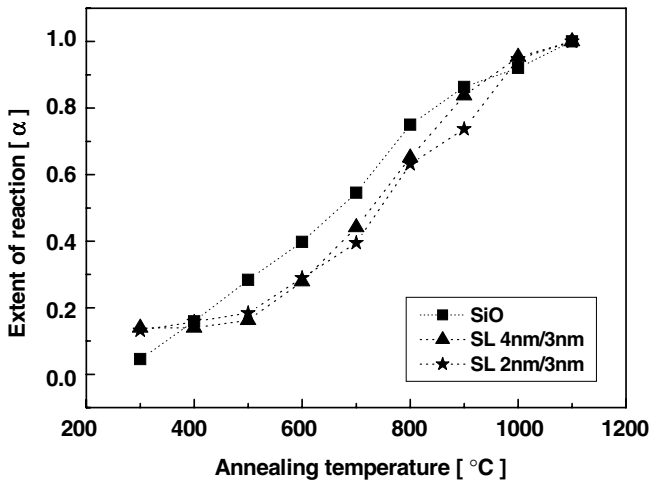

Figure 4. The extent of the reaction (α) for bulk SiO and SiO/SiO$_2$ superlattice samples (samples A and B) as a function of annealing temperature.

reaction (1) happens in the first seconds of the annealing process and that the α value is mainly influenced by the annealing temperature.

Please note that for nominal SiO$_2$ we also observe a slight shift from ν_i to ν_m (see figure 3) which cannot be directly attributed to changes in the composition and has therefore not been incorporated in figure 4.

3.2. Photoluminescence

Figure 5 demonstrates the PL spectra at different annealing temperatures for sample B (SL 4 nm/3 nm). Three different luminescence bands can be distinguished. A band at 2.2 eV is observed which shows an increasing PL intensity with increasing T_a up to 400 °C and a decreasing intensity for higher annealing temperatures (see figure 6). This band is not detectable any longer for samples with an annealing temperature above 800 °C. The PL maximum position does not show any significant change with annealing temperature. A second luminescence band appears which gradually shifts from a position of 1.7–1.4 eV as the annealing temperature increases from 300 to 900 °C. The PL intensity of this band is weaker than that of the first luminescence band but varies from sample to sample. Finally a Gaussian shaped strong luminescence is observed for temperatures above 900 °C with a peak position clearly dependent on the SiO layer thickness, i.e. 1.55 eV for sample A and 1.35 eV for sample B. A significantly broader non-Gaussian peak centred around 1.3 eV is observed for the bulk (100 nm) SiO film reflecting the broader and asymmetric size distribution of the Si nanocrystals.

The peak positions of PL bands I, II and III as a function of annealing temperature for the bulk SiO film and the samples A and B have similar behaviours, as shown in figure 7. For the bulk SiO$_2$ sample, no PL signal was detected under the conditions described.

4. Discussion

Combining annealing temperature dependent PL and FTIR measurements, the phase separation of thin SiO layers in the annealed SiO/SiO$_2$ superlattice can be divided into three processes:

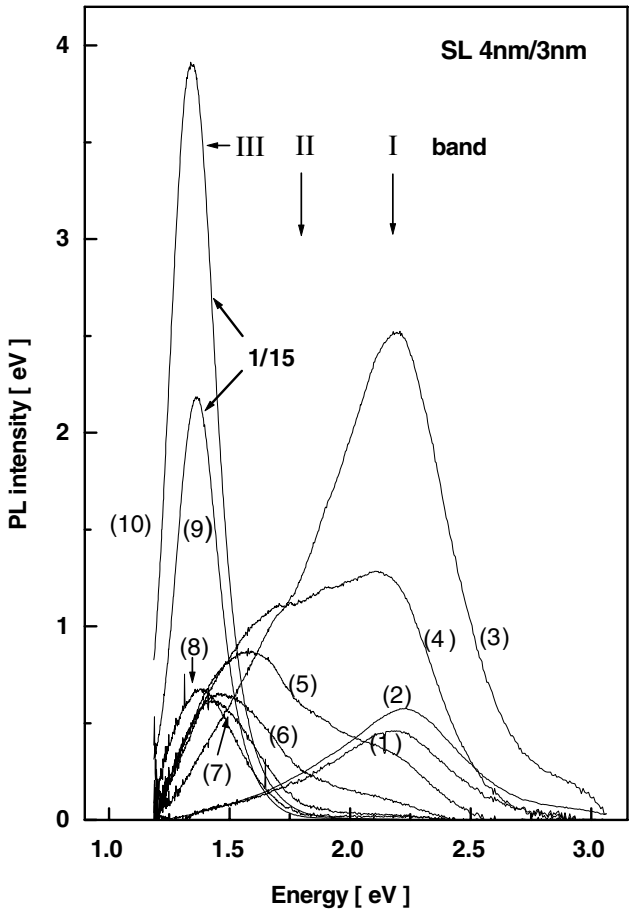

Figure 5. Photoluminescence of the annealed SiO/SiO_2 superlattice (sample B) showing the signatures of the different phase separation states assigned to the different annealing temperatures. Curve (1) corresponds to the PL spectrum of the as-prepared sample, curves (2)–(10) to the PL spectra of the 300–1100 °C annealed samples, respectively.

- Process 1, the rearrangement of the SiO into the SiO_2 structure, is characterized by an energetic shift of the Si–O–Si stretching mode (IR band III) and a variation of the PL intensity at 2.2 eV (PL band I) with a corresponding 880 cm^{-1} IR absorption intensity (IR band II).
- Process 2, the amorphous cluster growth, is characterized by the development of a second PL band (II) which gradually shifts its position from 1.7 to 1.4 eV with annealing temperature.
- Process 3, the crystallization of the amorphous clusters, is observed for annealing temperatures above 900 °C and characterized by a strong red luminescence (PL band III) with a constant peak position. No further changes in the Si–O related absorption band (IR band III) occur. Si nanocrystals are observed in the former SiO layer [6].

Processes 1 and 2 occur in parallel over the temperature range of 300–900 °C. Above 900 °C only process 3 proceeds.

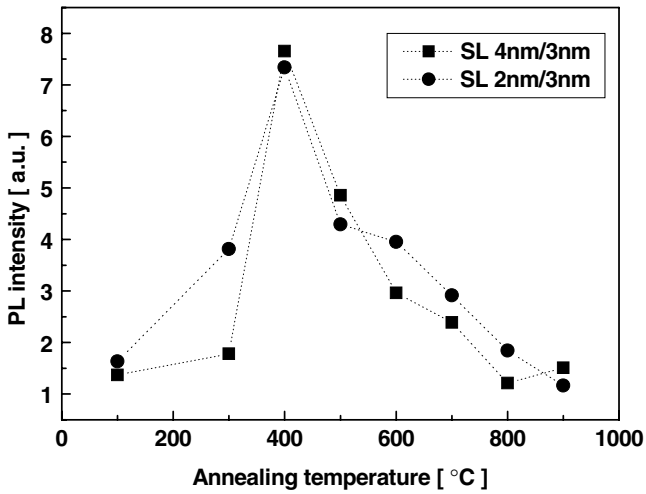

Figure 6. The annealing temperature dependence of the PL band I intensity for SiO/SiO_2 superlattice samples A and B.

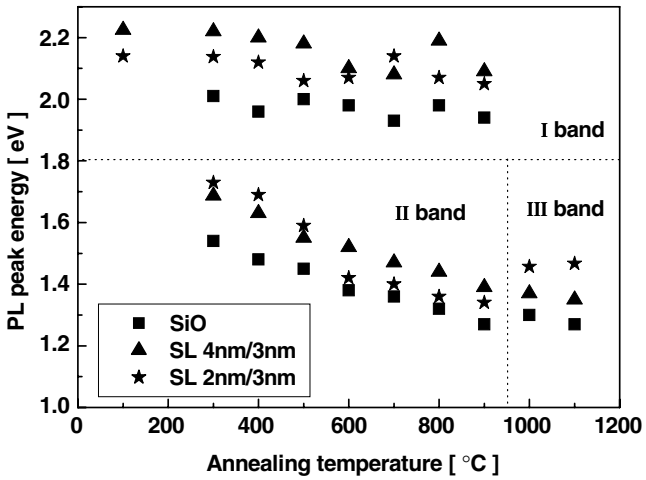

Figure 7. Peak energies of three PL bands as a function of the annealing temperature for bulk SiO and SiO/SiO_2 superlattice samples (samples A and B).

The rearrangement of the SiO happens in the first seconds of the annealing [12] and the extent of the reaction α is mainly given by the annealing temperature. This process is significantly characterized by the energetic shift of the Si–O–Si stretching mode. The peak position can be used to obtain a crude estimate of the stoichiometry for homogeneous SiO_x [13]. The position for the as-prepared bulk SiO was measured to be at 980 cm^{-1} and that of the as-prepared bulk SiO_2 at 1060 cm^{-1}. For the as-prepared film (100 °C) a position of 1039 cm^{-1} was found in the case of our superlattice samples A and B (figure 3), which is the contribution of both the SiO and SiO_2 layers. The difference in temperature dependence of the peak position for IR band III between the bulk SiO and the SiO_2 layer is obvious in figure 3, since in the case of the SiO_2 layer no phase separation happens. Only for temperatures above 700–800 °C does a rearrangement or a density compression of the SiO_2 seem to occur.

However, the deconvolution of the Si–O–Si stretching mode of the as-prepared superlattices into the SiO and SiO_2 parts cannot be accomplished in a simple way. Due to the large number of SiO_2 interfaces and the ultrathin layers, neither the effective medium nor the Brüggeman theory is valid for the superlattice system. Hence, the shift of the mode is only a qualitative measure for the process of the phase separation (figure 4). The 880 cm^{-1} absorption mode (figure 1) has been discussed in the literature as a mode related to $(SiO)_n$ rings isolated by oxide [9]. Theoretical studies [11, 14] indicated a non-bridging oxygen hole centre (NBOHC: $O_3{\equiv}Si–O\bullet$) situated on Si_6 rings as the origin of the IR absorption mode described and of a luminescence signal at about 1.9 eV. Skuja [15] proposed a model that assigns the excitation or recombination centre at 2 eV to the NBOHC, which has been supported by calculations of the electronic structure and vibrational calculation and is supported by the work of Galeener *et al* [16], too. It describes the PL itself and also its strong coupling to a localized Si–O stretching vibration. Ghislotti *et al* [17] and Rinnert *et al* [18] reported an increasing number of radiative defects produced by the ion implantation. Liao *et al* [19] proposed that the band is associated with the so-called E′ centre defects ($O_3{\equiv}Si\bullet$) and the defect density decreases with thermal annealing. Choi *et al* [20] also observed a yellow light emission from thermally grown silicon dioxide films and suggested that the emission originates from the radiative decay of self-trapped excitons.

Although similar IR and PL bands have been reported for siloxene [21, 22], we can exclude siloxene from consideration as the origin because our superlattice did not contain any hydrogen due to the high vacuum evaporation of the SiO powder and the inert gas (N_2) annealing process used. The similarity of the temperature behaviours of the intensities of the IR absorption and PL indicates the same origin for the two bands. The theoretical studies in [11, 15] assigning both modes to an NBOHC on a Si_6 ring structure support this interpretation. This means that the rearrangement of the SiO structure (process I) can be described as the synthesis of substoichiometric SiO_x accompanied by the formation of defects (e.g. NBOHC in combination with Si_6 rings), which vanish for higher annealing temperatures.

In process 2, the development of PL band II (1.7–1.4 eV) with decreasing emission energy for increasing T_a is observed. Similar PL spectra for amorphous Si/SiO_2 superlattices prepared by rf magnetron reactive sputtering from a silicon target in argon gas were observed by Liu *et al* [23]. The process of the Si cluster formation in SiO_x films for annealing at 750–950 °C was also reported by Furukawa *et al* [24] and was well supported by the results of Kanzawa *et al* [25]. Their samples, prepared by RF co-sputtering of Si and SiO_2, exhibited a broad PL band in the visible region (1.6–1.9 eV). The PL peak shows a red-shift with increasing annealing temperature and increasing Si concentration. The theoretical study [26] of Si clusters also shows that the average HOMO (highest occupied molecular orbital)–LUMO (lowest unoccupied molecular orbital) gap has a blue-shift in the range of 3–0.7 eV with reduction in cluster size. In our samples, we clearly see the development of amorphous clusters and an increase of the amorphous cluster size in the TEM images [27] from 300 to 900 °C which agrees perfectly with the observed red-shift of the PL (band II in figure 7).

Process 3 is characterized by the presence of nc-Si above 900 °C and a surrounding SiO_2 matrix which leads to a stable 1080 cm^{-1} FTIR signal and the appearance of a very strong PL signal originating from quantum confinement [6]. Above 900 °C the crystallization of the amorphous clusters into Si nanocrystals takes place, which can clearly be seen in dark field TEM and HRTEM investigations [6]. The fixed position of the PL above 900 °C reflects that the size of the Si nanocrystals is determined by the former cluster size. The quantum confinement origin for this strong room temperature luminescence has been discussed elsewhere [6]. The clear dependence of the PL peak position on the SiO layer thickness (figure 7) shows once more the possibility of size control via the SiO layer thickness.

Using our model of three processes a comprehensive understanding of the phase separation and crystallization processes was developed showing that the different and seemingly contradictory observations in the literature can be understood on the basis of different states of the network reorganization during phase separation and crystallization.

5. Conclusions

Comparing bulk SiO, SiO_2 and superlattice samples, the phase separation of ultrathin SiO_x layers in amorphous SiO/SiO_2 superlattices was studied over an annealing temperature range of 300 to 1100 °C by combination of PL and FTIR investigations. Three processes could be distinguished during the phase separation process: the transformation of the SiO into an SiO_2 network accompanied by the formation of NBOHC on Si ring structures, the growth of amorphous Si clusters in the annealing temperature range between 300 and 900 °C and the crystallization of these amorphous Si clusters above 900 °C. The size of the resulting Si nanocrystals is predetermined by the amorphous cluster size, i.e. by the SiO layer thickness. NBOHC, amorphous Si clusters and Si nanocrystals are different states of a non-stoichiometric SiO_x matrix having typical signatures in IR absorption and PL during annealing.

Acknowledgments

This work was financially supported by the German Research Foundation (DFG) and the Volkswagen Stiftung.

References

[1] Lehmann V and Gösele U 1991 *Appl. Phys. Lett.* **58** 856
[2] Canham L T 1990 *Appl. Phys. Lett.* **57** 1046
[3] Shimizu-Iwayama T, Hole D E and Boyd I W 1999 *J. Phys.: Condens. Matter* **11** 6595
[4] Hayashi S and Yamamoto K 1996 *J. Lumin.* **70** 352
[5] Kahler U and Hofmeister H 2001 *Opt. Mater.* **17** 83
[6] Zacharias M, Heitmann J, Scholz R, Kahler U, Schmidt M and Bläsing J 2002 *Appl. Phys. Lett.* **80** 661
[7] Tsu D V, Lucovsky G and Davidson B N 1989 *Phys. Rev.* B **40** 1795
[8] Zacharias M, Dimova-Malinovska D and Stutzmann M 1996 *Phil. Mag.* B **73** 799
[9] Kriegsmann H 1959 *Z. Anorg. Allg. Chem.* **298** 232
[10] Belot V, Corriu R J P, Leclercq D, Lefevre P, Mutin P H, Vioux A and Flank A M 1991 *J. Non-Cryst. Solids* **127** 207
[11] Hajnal Z, Deak P, Köhler Th, Kaschner R and Frauenheim Th 1998 *Solid State Commun.* **108** 93
[12] Hinds B J, Wang F, Wolf D M, Hinkle C L and Lucovsky G 1998 *J. Vac. Sci. Technol.* B **16** 2171
[13] Stolze F, Zacharias M, Schippel S and Garke B 1993 *Solid State Commun.* **87** 805
[14] Heitmann J and Lichtenberger O 2003 unpublished
[15] Skuja L 1992 *Solid State Commun.* **84** 613
[16] Galeener F L, Kerwin D B, Miller A J and Mikkelsen J C 1990 *Appl. Phys. Lett.* **57** 1046
[17] Ghislotti G, Nielsen B, Asoka-Kumar P, Lynn K G, Di Mauro L F, Bottani C E, Corni F, Tonini R and Ottaviani G P 1997 *J. Electrochem. Soc.* **144** 2196
[18] Rinnert H, Vergnat M, Marchal G and Burneau A 1999 *J. Lumin.* **80** 445
[19] Liao L S, Bao X M, Li N S, Zheng X Q and Min N B 1996 *J. Lumin.* **68** 199
[20] Choi W C, Lett M-S, Kim E K, Kim C K, Min S-K, Park C-Y and Lee J Y 1996 *Appl. Phys. Lett.* **69** 3402
[21] Dettlaff-Weglikowska U, Hönle W, Molassioti-Dohms A, Finkbeiner S and Weber J 1997 *Phys. Rev.* B **56** 13132
[22] Friedman S L, Marcus M A, Adler D L, Xie Y H, Harris T D and Citrin P H 1993 *Appl. Phys. Lett.* **62** 1934
[23] Liu N N, Sun J M, Pan S H, Chen Z H, Wang R P, Shi W S and Wang X G 2000 *Superlatt. Microstruct.* **28** 157
[24] Furukawa K, Liu Y, Nakashima H, Gao D, Uchino K, Muraoka K and Tsuzuki H 1992 *Appl. Phys. Lett.* **61** 2446
[25] Kanzawa Y, Hayashi S and Yamamoto K 1996 *J. Phys.: Condens. Matter* **8** 4823
[26] Allan G, Delerue C and Lannoo M 1997 *Phys. Rev. Lett.* **78** 3161
[27] Yi L X, Heitmann J, Scholz R and Zacharias M 2002 *Appl. Phys. Lett.* **81** 4248